ZF Detectors over Correlated K Fading MIMO Channels

Michail Matthaiou, *Member, IEEE*, Nestor D. Chatzidiamantis, *Student Member, IEEE*, George K. Karagiannidis, *Senior Member, IEEE*, and Josef A. Nossek, *Fellow, IEEE*

***Abstract*—This paper provides a systematic characterization of Zero-Forcing (ZF) detectors over multiple-input multiple-output (MIMO) channels that experience both small and large-scale fading. In particular, we consider the generic K distribution (Rayleigh/gamma distribution) to model the composite fading fluctuations and also assume the general case of semi-correlated small-scale fading. In the following, novel exact analytical expressions for the achievable sum rate are derived, followed by asymptotic expressions in the high and low Signal-to-Noise ratio (SNR) regimes. In these limiting cases, two common and insightful affine expansions are studied followed by new, closed-form upper and lower bounds on the sum rate that remain tight for all SNRs. In the second part of the paper, we present exact tractable expressions along with first-order expansions for the symbol error rate (SER) and outage probability; we also quantify the performance of ZF detectors in terms of diversity order and array (or coding) gain. The implications of the model parameters on the ZF detector performance are investigated via Monte-Carlo simulations which also validate the theoretical analysis.**

***Index Terms*—Zero-forcing detection, multiple-input multiple-output (MIMO) systems, performance analysis, sum rate, correlated fading.**

I. Introduction

THE capacity of point-to-point multiple-input multiple-output (MIMO) systems has been thoroughly investigated over the past decade under Rayleigh fading conditions and assuming all different types of spatial correlation [1]–[5]. When MIMO technology is combined with the classical principle of distributed antenna systems [6], [7], then we end up with the so-called distributed MIMO (D-MIMO) systems which exploit both spatial micro and macro-diversity [8]–[11]. The main feature of these systems is that multiple antennas at one end of the wireless channel are packed into multiple radio ports that are spatially separated (e.g. in an uplink scenario, ports are placed at different locations and communicate with the base station). Hence, each link experiences different degree of path loss, as a result of the different access distances, along with different shadowing effects. We recall that the latter manifestation is rather critical when assessing MIMO performance since it can significantly diminish the benefits of MIMO technology.

In the analysis of composite fading channels, it is well known that the most common propagation model is the Rayleigh/lognormal (RLN) model which has been extensively used to approximate the fading fluctuations in radar and RF communication systems [12], [13]. It is also the prevalent model in the characterization of composite fading MIMO channels (see for instance [8]–[11], [14]–[16] and references therein). The main disadvantage of the RLN model though is that the composite probability density function (PDF) is not in closed-form, and consequently, the most important figures of merit, such as the ergodic capacity and symbol error rate (SER), can not be easily evaluated. On this basis, the lognormal shadowing was approximated by the analytically friendlier Gamma shadowing; a theoretical justification for this choice, using a set of empirical data, can be found in [17]. The resulting fading model is referred to as the K-distribution [17], [18], which will serve as our reference model henceforth.

In this paper, we are mainly interested in the performance analysis of Zero-Forcing (ZF) linear receivers over such composite D-MIMO channels. We recall that a ZF receiver induces lower complexity compared to other receivers like successive interference cancelation (SIC) or minimum mean-squared error (MMSE) but, when independent decoding is used, it suffers from an inherent noise enhancement [19]. Conceptually, most studies dealing with the performance assessment of these detectors are limited to MIMO channels experiencing only small-scale fading, e.g. semi-correlated Rayleigh [20], [21], doubly-correlated Rayleigh [22], uncorrelated Ricean [23] and semi-correlated Ricean fading [24]. To the best of the authors' knowledge, the only relevant study in the context of composite fading was recently reported in [16], where the authors examined the achievable sum rate of ZF detectors over RLN MIMO channels. The main disadvantage of this approach is that the final sum rate result is given in integral form (see [16, Eq. (15)]). In order to circumvent this, the authors approximated the sum rate numerically via Gauss-Hermite polynomials with this technique, however, being time-consuming (especially at low Signal-to-Noise ratios (SNRs)) and not amenable to further manipulations. In addition, that analysis was limited to co-located MIMO (C-MIMO) antenna arrays and, consequently, does not consider the benefits offered by D-MIMO.

In light of this fact, we hereafter pursue a statistical analysis

Paper approved by N. C. Beaulieu, the Editor for Wireless Communication Theory of the IEEE Communications Society. Manuscript received May 28, 2010; revised October 5, 2010.

Part of this paper has been presented at the IEEE International Conference on Acoustics, Speech and Signal Processing (ICASSP), Prague, Czech Republic, May 2011.

M. Matthaiou was with the Institute for Circuit Theory and Signal Processing, Technische Universität München (TUM), Germany. He is now with the Department of Signals and Systems, Chalmers University of Technology, SE-412 96, Gothenburg, Sweden (e-mail: michail.matthaiou@chalmers.se).

N. D. Chatzidiamantis and G. K. Karagiannidis are with the Department of Electrical and Computer Engineering, Aristotle University of Thessaloniki, 54 124, Thessaloniki, Greece (e-mail: {nestoras, geokarag}@auth.gr).

J. A. Nossek is with the Institute for Circuit Theory and Signal Processing, Technische Universität München (TUM), Arcistrasse 21, 80333, Munich, Germany (e-mail: nossek@nws.ei.tum.de).

Digital Object Identifier 10.1109/TCOMM.2011.041111.100321

of ZF detectors over composite K MIMO channels and also consider the more general case of correlated Rayleigh fading with correlation on the side with the minimum number of antennas. Our analysis encompasses both the sum rate along with the SER and outage probability. In particular, the paper contributions can now be summarized as follows:

- We first extend and complement some recent results on single-antenna systems to the case of D-MIMO systems under composite correlated K fading. This extension leads to new, analytical expressions for the statistics of the instantaneous SNR at the output of the ZF detector. The resulting cumulative density function (CDF) expression is given in terms of a Meijer's-G function which can be easily evaluated and efficiently programmed in most standard software packages (e.g. MAPLE, MATHEMATICA). We also present alternative simplified CDF formulas for both integer and non-integer values of the shape parameter of gamma fading.
- The exact achievable sum rate of a ZF detector over correlated K MIMO channels is analytically derived along with tractable expressions in the asymptotically high and low-SNR regimes. In these asymptotic cases, two affine sum rate expansions are investigated based on the notions of *high-SNR slope*, *high-SNR power offset* along with the *minimum energy per bit* and *wideband slope*. In addition, we propose novel, closed-form upper and lower bounds on the sum rate. These expressions yield useful insights into the implications of the model parameters on the ZF detector's performance.
- In the second part of the paper, we focus on the SER and outage probability measures for which exact analytical expressions along with first-order expansions around the origin are deduced. Moreover, we use a common parametrization in the area of wireless communications to quantify the ZF performance in terms of *diversity order* and *array (or coding) gain*.

The remainder of the paper is organized as: In Section II, the MIMO system model used throughout the paper is introduced and the PDF/CDF of the instantaneous ZF SNR are derived. In Section III, we provide new, analytical expressions for the achievable sum rate along with a detailed high and low-SNR analysis and upper/lower bounds. A similar analysis in terms of SER and outage probability is performed in Section IV. A set of numerical results is given in Section V in order to explore the implications of the model parameters on the proposed theoretical expressions while Section VI concludes the paper and summarizes the key findings.

Notation: We use upper and lower case boldface to denote matrices and vectors, respectively. The sets of complex and real numbers are respectively expressed via $\mathbb{C}$ and $\mathbb{R}$. The $n \times n$ identity matrix reads as $\mathbf{I}_n$. The expectation is given by $\mathbb{E}[\cdot]$, the variance by $\mathrm{Var}[\cdot]$ while the matrix determinant by $\det(\cdot)$. The symbols $(\cdot)^{\dagger}$ and $(\cdot)^{H}$ represent the pseudo-inverse and Hermitian transpose of a matrix, respectively while $\mathrm{diag}(\cdot)$ generates a diagonal matrix.

II. MIMO System Model and SNR Statistics

Let us consider a typical uplink D-MIMO system equipped with N_r receive antennas and L radio ports each connected to N_t transmit antennas and also require that $N_r \geq LN_t$. In the following, we assume that the receiver has perfect channel state information (CSI) while the transmitter knows neither the statistics nor the instantaneous CSI. Then, in a typical spatial multiplexing system, a sensible choice for the transmitter is to equally split the available average power, P, amongst all data streams. In the case of composite fading (i.e. small and large-scale fading), the input-output relationship is

$$\mathbf{y} = \sqrt{\frac{P}{LN_t}}\mathbf{H}\boldsymbol{\Xi}^{1/2}\mathbf{s} + \mathbf{n} \tag{1}$$

where $\mathbf{y} \in \mathbb{C}^{N_r \times 1}$ is the received signal vector, $\mathbf{s} \in \mathbb{C}^{LN_t \times 1}$ is the vector containing the transmitted symbols which are drawn from a unit-power constellation while the complex AWGN term is zero-mean with covariance $\mathbb{E}\left[\mathbf{n}\mathbf{n}^H\right] = N_0\mathbf{I}_{N_r}$, where N_0 is the noise power.

The entries of the diagonal matrix $\boldsymbol{\Xi} \in \mathbb{R}^{LN_t \times LN_t}$ represent the large-scale effects, and hence $\boldsymbol{\Xi} = \mathrm{diag}\left\{\mathbf{I}_{N_t}\xi_m / D_m^{\upsilon}\right\}_{m=1}^{L}$ where D_m denotes the normalized distance (with a reference distance equal to 1 km) between the receiver and the m-th radio port, while υ is the path-loss exponent with typical values ranging from $2-6$. The large-scale fading coefficients $\xi_m, m = 1, \ldots, L$, are modeled as gamma random variables (RVs), or

$$f_{\xi_m}(\xi_m) = \frac{\xi_m^{k_m - 1}}{\Gamma(k_m)\Omega_m^{k_m}} \exp\left(-\frac{\xi_m}{\Omega_m}\right), \quad \xi_m, \Omega_m, k_m \geq 0 \tag{2}$$

where k_i, $\Omega_i = \mathbb{E}[\xi_i]/k_i$, are the so-called shape and scale parameters of the gamma distribution respectively, while $\Gamma(\cdot)$ is the well-known gamma function. As was previously mentioned, the small-scale fading is assumed to follow a semi-correlated Rayleigh distribution and as such, we can express $\mathbf{H} \in \mathbb{C}^{N_r \times LN_t}$ according to $\mathbf{H} = \mathbf{H}_w\mathbf{R}_t^{1/2}$, where the entries of $\mathbf{H}_w$ are modeled as i.i.d. $\mathcal{CN}(0,1)$ RVs while $\mathbf{R}_t$ is the positive definite covariance matrix of every row of $\mathbf{H}$. Note that small-scale fading correlation occurs only between the antennas of the same radio port since the L ports are, in general, well separated in space.

After defining $\mathbf{Z} \triangleq \mathbf{H}\boldsymbol{\Xi}^{1/2}$, we can apply the concept of ZF reception on (1) to obtain the ZF filter matrix according to $\mathbf{G} = (P/LN_t)^{-1/2}\mathbf{Z}^{\dagger}$ [19]. Thus, the received signal after detection, which is used to recover the spatially multiplexed data streams, becomes

$$\hat{\mathbf{s}} = \mathbf{G}\mathbf{y} = \mathbf{s} + \left(\frac{P}{LN_t}\right)^{-1/2}\mathbf{Z}^{\dagger}\mathbf{n}. \tag{3}$$

It should be noted that the noise term is now colored and as such the components of $\hat{\mathbf{s}}$ are in general not independent. Yet, introducing the simple detection scheme of [20], we consider that each component of $\hat{\mathbf{s}}$ is independently decoded. Then, the received signal is decomposed into LN_t parallel streams with the instantaneous received SNR at the m-th ZF output ($1 \leq m \leq LN_t$) being equal to

$$\gamma_m \triangleq \frac{\rho}{LN_t\left[\left(\mathbf{Z}^H\mathbf{Z}\right)^{-1}\right]_{mm}} = \frac{\rho\left[\boldsymbol{\Xi}\right]_{mm}}{LN_t\left[\left(\mathbf{H}^H\mathbf{H}\right)^{-1}\right]_{mm}} \tag{4}$$

where $\rho = P/N_0$ is the average SNR and $[\cdot]_{mm}$ returns the m-th diagonal element of a matrix, while the second equality

$$F_{\gamma_m}(\gamma_{\text{th}}) = \frac{\pi \csc(\pi(N_r - LN_t + 1 - k_m))}{(N_r - LN_t)!\Gamma(k_m)} \left(\frac{LN_t D_m^v \sigma_m}{\rho \Omega_m}\gamma_{\text{th}}\right)^{N_r - LN_t + 1} \times \left(\frac{\left(\frac{LN_t D_m^v \sigma_m}{\rho\Omega_m}\gamma_{\text{th}}\right)^{k_m - N_r + LN_t - 1} {}_1F_2\left(k_m; 1 + k_m, k_m - N_r + LN_t; \frac{LN_t D_m^v \sigma_m}{\rho\Omega_m}\gamma_{\text{th}}\right)}{k_m \Gamma(k_m - N_r + LN_t)} - \frac{{}_1F_2\left(N_r - LN_t + 1; N_r - LN_t + 2, N_r - LN_t + 2 - k_m; \frac{LN_t D_m^v \sigma_m}{\gamma\Omega_m}\gamma_{\text{th}}\right)}{(N_r - LN_t + 1)\Gamma(N_r - LN_t + 2 - k_m)} \right). \quad (9)$$

follows from the fact that $\boldsymbol{\Xi}$ is diagonal. In order to simplify the following manipulations, we can now define the random small-scale counterpart as follows

$$x_m = \frac{1}{\left[(\mathbf{H}^H\mathbf{H})^{-1}\right]_{mm}}, \; m = 1, \ldots, LN_t \quad (5)$$

which follows a complex semi-correlated central Wishart distribution $x_m \sim \mathcal{CW}(N_r - LN_t + 1, 1/[\mathbf{R}_t^{-1}]_{mm})$ and its PDF was explicitly given in [20, Theorem 1]

$$f_{x_m}(x_m) = \frac{\sigma_m e^{-x_m\sigma_m}}{(N_r - LN_t)!}(x_m\sigma_m)^{N_r - LN_t} \quad (6)$$

where σ_m is the m-th diagonal entry of $\mathbf{R}_t^{-1}$. The following theorem returns in closed-form the PDF/CDF of the instantaneous SNR of a ZF detector over K MIMO channels. We note that these expressions will be particularly useful when analyzing the performance of ZF detectors in terms of sum rate and SER.

Theorem 1: The PDF/CDF of the instantaneous SNR γ_m in (4), are respectively given by

$$f_{\gamma_m}(\gamma_m) = \frac{2K_{N_r - LN_t - k_m + 1}\left(2\sqrt{\frac{LN_t D_m^v \sigma_m}{\rho\Omega_m}\gamma_m}\right)}{(N_r - LN_t)!\Gamma(k_m)} \times \left(\frac{LN_t D_m^v \sigma_m}{\rho\Omega_m}\right)^{\frac{N_r - LN_t + k_m + 1}{2}} \gamma_m^{\frac{N_r - LN_t + k_m - 1}{2}} \quad (7)$$

$$F_{\gamma_m}(\gamma_{\text{th}}) = \frac{1}{(N_r - LN_t)!\Gamma(k_m)} \times G_{1,3}^{2,1}\left[\frac{LN_t D_m^v \sigma_m}{\rho\Omega_m}\gamma_{\text{th}} \middle| \begin{matrix} 1 \\ N_r - LN_t + 1, k_m, 0 \end{matrix}\right] \quad (8)$$

where γ_{th} is the SNR threshold, $K_\nu(\cdot)$ is the ν-th order modified Bessel function of the second kind [25, Eq. (8.407.1)], while $G_{p,q}^{m,n}\left[x, \left|\begin{matrix}\alpha_1,\ldots,\alpha_p \\ \beta_1,\ldots,\beta_q\end{matrix}\right.\right]$ is the Meijer's G-function [25, Eq. (9.301)].

Proof: A detailed proof is given in Appendix A. ∎

Note that similar expressions were originally derived in [26], in the context of single-antenna systems and yet were limited to the special case of uncorrelated Rayleigh fading. We now present two alternative simplified CDF expressions depending on the values of the shape parameter of gamma-fading:

Corollary 1: The CDF of the instantaneous SNR γ_m in (4), can be alternatively expressed as:

- When $k_m \notin \mathbb{Z}$ we get (9) at the top of the page, where ${}_pF_q(\cdot)$ denotes the generalized hypergeometric function, with p, q being non-negative integers [25, Eq. (9.14.1)].
- When $k_m \in \mathbb{Z}$

$$F_{\gamma_m}(\gamma_{\text{th}}) = 1 - \sum_{\ell=0}^{k_m - 1} \frac{2\left(\frac{LN_t D_m^v \sigma_m}{\rho\Omega_m}\right)^{\frac{N_r - LN_t + \ell + 1}{2}}}{(N_r - LN_t)!(k_m - \ell)!} \times \gamma_{\text{th}}^{\frac{N_r - LN_t + \ell + 1}{2}} K_{N_r - LN_t + 1 - \ell}\left(2\sqrt{\frac{LN_t D_m^v \sigma_m}{\rho\Omega_m}\gamma_{\text{th}}}\right). \quad (10)$$

Proof: A detailed proof is relegated in Appendix B. ∎

As an interesting example of the usefulness of the above expressions, we can consider the per-subchannel amount of fading (AF) which is a unified measure of the severity of fading, defined as the ratio of variance of the received energy to the square of the average received energy [13, Eq. (1.27)],

$$\text{AF}_{\gamma_m} \triangleq \frac{\text{Var}[\gamma_m]}{(\mathbb{E}[\gamma_m])^2} = \frac{k_m + N_r - LN_t + 2}{k_m(N_r - LN_t + 1)}. \quad (11)$$

For the evaluation of the required statistics we have used (7) and the integral identity [25, Eq. (6.561.16)]. Note that the AF is a monotonic decreasing function of the shadowing shape parameter k_m, since $\frac{d\text{AF}_{\gamma_m}}{dk_m} = -\frac{N_r - LN_t + 2}{k_m^2(N_r - LN_t + 1)} < 0$, and independent of the scale parameter, spatial correlation and terminal distances.

III. Achievable Sum Rate of ZF Detectors

In this section, we elaborate on the sum rate performance of ZF detectors and provide analytical expressions for the exact and asymptotic SNR regimes.

A. Exact Analysis

As a starting point, we determine the achievable sum rate, assuming independent decoding at the receiver, as

$$R \triangleq \sum_{m=1}^{LN_t} \mathbb{E}[\log_2(1 + \gamma_m)] = \sum_{m=1}^{LN_t} \mathbb{E}\left[\log_2\left(1 + \frac{\rho}{LN_t}\frac{\xi_m x_m}{D_m^v}\right)\right] \quad (12)$$

where the expectation is taken over all channel realizations of $\mathbf{H}$ and $\boldsymbol{\Xi}$ and the channel is assumed to be ergodic. The following theorem returns an analytical expression for the exact sum rate of ZF detectors over correlated K MIMO channels and constitutes the key contribution of this paper:

Theorem 2: The achievable sum rate of ZF detectors over correlated K MIMO channels is given by

$$R = \frac{1}{\ln 2 (N_r - LN_t)!} \sum_{m=1}^{LN_t} \frac{1}{\Gamma(k_m)} \times G_{4,2}^{1,4}\left[\frac{\rho \Omega_m}{LN_t \sigma_m D_m^v} \middle| \begin{matrix} 1-k_m, LN_t - N_r, 1, 1 \\ 1, 0 \end{matrix} \right]. \quad (13)$$

Proof: The proof starts by expressing the expectation in (12) in integral form as

$$R = \frac{1}{\ln 2} \sum_{m=1}^{LN_t} \int_0^\infty \int_0^\infty \ln\left(1 + \frac{\rho \xi_m x_m}{LN_t D_m^v}\right) \times f_{\xi_m}(\xi_m) f_{x_m}(x_m) d\xi_m dx_m. \quad (14)$$

Substituting (2) and (6) into (14) and successively applying [25, Eq. (7.813.1)], we can obtain (13) after some basic algebraic manipulations. ∎

For i.i.d. Rayleigh fading conditions (i.e. $L = 1$, $\sigma_m = 1$, $\mathbf{\Xi} = \mathbf{I}_{N_t}$), (13) reduces to

$$R = \left(\frac{N_t}{\rho}\right)^{N_r - N_t + 1} \frac{N_t e^{\frac{N_t}{\rho}}}{\ln 2} \times \sum_{m=1}^{N_r - N_t + 1} \left(\frac{\rho}{N_t}\right)^m \Gamma\left(m - N_r + N_t - 1, \frac{N_t}{\rho}\right) \quad (15)$$

where $\Gamma(\alpha, x) = \int_x^\infty t^{\alpha-1} e^{-t} dt$ is the upper incomplete gamma function [27, Eq. (6.5.3)]. Note that (15) coincides with [28, Eq. (6)]. Although the general expression in (13) can be easily evaluated[1], it does not offer useful insights into the implications of the model parameters on the sum rate. To this end, we consider the infinitely high and low-SNR regimes.

B. High-SNR Analysis

In this case ($\rho \to \infty$), we can first obtain the following straightforward result:

Corollary 2: The achievable sum rate of ZF detectors over correlated K MIMO channels, at high SNRs, is given by

$$R^\infty = LN_t \log_2\left(\frac{\rho}{LN_t}\right) + \frac{LN_t}{\ln 2} \psi(N_r - LN_t + 1) - \sum_{m=1}^{LN_t} \log_2(\sigma_m) + N_t \sum_{m=1}^{L} \left(\frac{\psi(k_m)}{\ln 2} + \log_2\left(\frac{\Omega_m}{D_m^v}\right)\right) \quad (16)$$

where $\psi(x)$ is the digamma function [25, Eq. (8.360.1)].

Proof: The result follows by taking ρ large in (14), then using the integral identity [25, Eq. (4.352.1)]

$$\int_0^\infty x^{\nu-1} e^{-\mu x} \ln x dx = \frac{\Gamma(\nu)}{\mu^\nu} (\psi(\nu) - \ln \mu) \quad \mathrm{Re}(\mu, \nu) > 0$$

and simplifying the resulting expression. ∎

The above expression is quite intuitive since it indicates that at high SNRs the effects of small and large-scale fading are decoupled, which is consistent with the results in [10], [11], [15]. We also validate the diminishing effects of spatial correlation on the sum rate since, due to Hadamard's inequality, $1 \le \det(\mathbf{R}_t^{-1}) \le \prod_{m=1}^{LN_t} \sigma_m$, with equality for $\mathbf{R}_t = \mathbf{I}_{LN_t}$. For i.i.d. Rayleigh fading, we can obtain via (16),

$$R^\infty = N_t \log_2\left(\frac{\rho}{N_t}\right) + \frac{N_t}{\ln 2} \psi(N_r - N_t + 1) \le N_t \log_2\left(\frac{\rho}{N_t}\right) + \frac{1}{\ln 2} \sum_{i=0}^{N_t - 1} \psi(N_r - i) \quad (17)$$

where the upper bound of (17) corresponds to the high-SNR ergodic capacity of a C-MIMO system with optimal receivers under $N_r \ge N_t$ [2, Eq. (12)], [3, Eq. (9)].

In order to get a better insight into the high-SNR sum rate performance, we can now invoke the following affine expansion of the achievable sum rate [30], [31][2]

$$R(\rho, N_r, L, N_t) = \mathcal{S}_\infty (\log_2 \rho - \mathcal{L}_\infty) + o(1) \quad (18)$$

where $\mathcal{S}_\infty$ is the so-called *high-SNR slope* in bits/s/Hz per 3-dB units

$$\mathcal{S}_\infty = \lim_{\rho \to \infty} \frac{R(\rho, N_r, L, N_t)]}{\log_2 \rho} \quad (19)$$

while $\mathcal{L}_\infty$ is the zero-th order term or *high-SNR power offset*, in 3-dB units, given by

$$\mathcal{L}_\infty = \lim_{\rho \to \infty} \left(\log_2 \rho - \frac{R(\rho, N_r, L, N_t)}{\mathcal{S}_\infty} \right). \quad (20)$$

Proposition 1: The high-SNR slope and power offset of ZF detectors over correlated K MIMO channels are respectively

$$\mathcal{S}_\infty = LN_t \quad (21)$$

$$\mathcal{L}_\infty(N_r, L, N_t) = \log_2(LN_t) - \frac{1}{\ln 2} \psi(N_r - LN_t + 1) + \frac{1}{LN_t} \sum_{m=1}^{LN_t} \log_2(\sigma_m) - \frac{1}{L} \sum_{m=1}^{L} \left(\frac{\psi(k_m)}{\ln 2} + \log_2\left(\frac{\Omega_m}{D_m^v}\right)\right). \quad (22)$$

Proof: The proof follows trivially by combining the high-SNR sum rate expression (16) with the definitions (19), (20). ∎

The relationship in (21) verifies the well-known characteristic of MIMO systems, that is the asymptotically (in terms of SNR) linear sum rate (or capacity) scaling with the minimum number of antennas [1]–[4]. In addition, (22) indicates that for a fixed number of transmit antennas, using more antennas at the receiver leaves the high-SNR slope unaffected but increases the high-SNR sum rate by reducing the power offset due to the additional power captured by every new receive antenna. In fact, for fixed L, N_t, adding n receive antennas would reduce the offset by

$$\delta(N_r, n) \triangleq \mathcal{L}_\infty(N_r + n, L, N_t) - \mathcal{L}_\infty(N_r, L, N_t) = -\frac{1}{\ln 2} \sum_{\ell = N_r - LN_t + 1}^{N_r - LN_t + n} \frac{1}{\ell} \quad (23)$$

where we have used the alternative definition of the digamma function from [25, Eq. (8.365.4)].

On the other hand, spatial correlation tends to logarithmically increase the power offset. We note that these observations

[1]Note that when the Meijer's G-function in (13) has non-integer arguments (i.e. $k_m \notin \mathbb{Z}$), it can be expanded as a finite weighted sum of hypergeometric/digamma functions following the generic approach of [29, Appendix I].

[2]We use the standard notation $f(x) = o(g(x)), g(x) > 0$ to state that $f(x)/g(x) \to 0$ as $x \to \infty$.

are consistent with the results originally presented in [31]. It is finally noteworthy that in the case of i.i.d. Rayleigh fading channels (21), (22) reduce to $\mathcal{S}_\infty = N_t, \mathcal{L}_\infty(N_r, N_t) = \log_2(N_t) - \frac{1}{\ln 2}\psi\left(N_r - N_t + 1\right)$ which are respectively identical with [32, Eq. (19)] and [32, Eq. (42)]; the latter have been derived in the context of MIMO MMSE receivers. This phenomenon is anticipated since at high-SNRs the ZF and MMSE detectors behave equivalently in terms of sum rate [19].

C. Low-SNR Analysis

We can now investigate the sum rate performance of ZF detectors in the power-limited (or wideband) regime. We begin by deriving a first-order Taylor expansion of the sum rate as $\rho \to 0$.

Corollary 3: The achievable sum rate of ZF detectors over correlated K MIMO channels, at low Signal-to-Noise ratios (SNRs), is given by

$$R^0 = \frac{\rho(N_r - LN_t + 1)}{LN_t \ln 2} \sum_{m=1}^{LN_t} \frac{k_m \Omega_m}{\sigma_m D_m^\upsilon}. \tag{24}$$

Proof: The proof starts by applying a first-order Taylor expansion of (12) around $\rho = 0^+$, to get

$$R^0 = \frac{1}{\ln 2}\frac{\rho}{LN_t} \sum_{m=1}^{LN_t} \mathbb{E}\left[\frac{\xi_m x_m}{D_m^\upsilon}\right] + o(\rho) \tag{25}$$

where we have used the property $\ln(1+x) \approx x$ when $x \to 0$. Substituting (2) and (6) into (25), and successively applying [25, Eq. (3.381.4)]

$$\int_0^\infty x^{\nu-1}\exp(-\mu x)dx = \frac{\Gamma(\nu)}{\mu^\nu}, \ \ \mathrm{Re}(\mu,\nu) > 0 \tag{26}$$

we can obtain (24) after appropriate simplifications. ∎

We note that for i.i.d. Rayleigh fading conditions, (24) simplifies to

$$R^0 = \frac{\rho(N_r - N_t + 1)}{N_t \ln 2} \leq \frac{\rho N_r}{\ln 2} \tag{27}$$

with the upper bound of (27) being the low-SNR ergodic capacity of a C-MIMO system with optimal receivers under $N_r \geq N_t$ [2, Eq. (23)]. The above formulas indicate that a higher N_r can significantly improve the ZF performance due to the additional power captured by the extra antennas and also due to the mitigation of noise enhancement effect.

Although the first-order expansion applied in the derivation of Corollary 3 is quite straightforward and insightful, it has been theoretically shown that it can lead to misleading results regarding the impact of the channel in the low-SNR (or wideband) regime [33], [34]. To this end, it is more meaningful to explore the low-SNR sum rate in terms of the normalized transmit energy per information bit E_b/N_0 rather than per-symbol SNR. This representation reads as

$$R\left(\frac{E_b}{N_0}\right) \approx \mathcal{S}_0 \log_2\left(\frac{\frac{E_b}{N_0}}{\frac{E_b}{N_{0\,\min}}}\right) \tag{28}$$

where $\frac{E_b}{N_{0\,\min}}$ and $\mathcal{S}_0$ are now the two key parameters determining the behavior in the low-SNR regime, corresponding to the "*minimum normalized energy per information bit required to convey any positive rate reliably*" and the *wideband slope*, respectively [33].

Proposition 2: The minimum energy per information bit and the wideband slope of ZF detectors over correlated K MIMO channels are respectively

$$\frac{E_b}{N_{0\,\min}} = \frac{LN_t \ln 2}{(N_r - LN_t + 1)}\left(\sum_{m=1}^{LN_t}\frac{k_m\Omega_m}{\sigma_m D_m^\upsilon}\right)^{-1} \tag{29}$$

$$\mathcal{S}_0 = \frac{2(N_r - LN_t + 1)}{(N_r - LN_t + 2)} \frac{\left(\sum_{m=1}^{LN_t}\frac{k_m\Omega_m}{\sigma_m D_m^\upsilon}\right)^2}{\sum_{m=1}^{LN_t} k_m(k_m+1)\left(\frac{\Omega_m}{\sigma_m D_m^\upsilon}\right)^2}. \tag{30}$$

Proof: From [33], we have that $\frac{E_b}{N_{0\,\min}}$ and $\mathcal{S}_0$ are respectively given by

$$\frac{E_b}{N_{0\,\min}} \triangleq \lim_{\rho\to 0}\frac{\rho}{R(\rho)} = \frac{1}{\dot{R}(0)} \ \ \text{and} \ \ \mathcal{S}_0 \triangleq -\frac{2\ln 2\left[\dot{R}(0)\right]^2}{\ddot{R}(0)} \tag{31}$$

where $\dot{R}(\cdot)$ and $\ddot{R}(\cdot)$ denote the first and second-order derivatives of the sum rate (12) over the SNR ρ. As such, substituting (12) into (31) and taking the first derivative w.r.t. ρ, we obtain

$$\begin{aligned}\dot{R}(0) &= \frac{1}{\ln 2}\sum_{m=1}^{LN_t}\mathbb{E}\left[\left.\frac{\frac{1}{LN_t}\frac{\xi_m x_m}{D_m^\upsilon}}{1+\frac{\rho}{LN_t}\frac{\xi_m x_m}{D_m^\upsilon}}\right|_{\rho=0}\right] \\ &= \frac{1}{LN_t \ln 2}\sum_{m=1}^{LN_t}\mathbb{E}\left[\frac{\xi_m x_m}{D_m^\upsilon}\right].\end{aligned} \tag{32}$$

In a similar manner, we can evaluate the second derivative as follows

$$\begin{aligned}\ddot{R}(0) &= -\frac{1}{\ln 2}\sum_{m=1}^{LN_t}\mathbb{E}\left[\left.\frac{\left(\frac{1}{LN_t}\frac{\xi_m x_m}{D_m^\upsilon}\right)^2}{\left(1+\frac{\rho}{LN_t}\frac{\xi_m x_m}{D_m^\upsilon}\right)^2}\right|_{\rho=0}\right] \\ &= -\frac{1}{\ln 2}\left(\frac{1}{LN_t}\right)^2\sum_{m=1}^{LN_t}\mathbb{E}\left[\left(\frac{\xi_m x_m}{D_m^\upsilon}\right)^2\right].\end{aligned} \tag{33}$$

Combining (32), (33) with the definitions in (31) and the relationship in (26), we can obtain the desired results in (29)–(30) after appropriate simplifications. ∎

For i.i.d. Rayleigh fading, it can be shown that $\frac{E_b}{N_{0\,\min}} = \ln 2/(N_r - N_t + 1)$ and $\mathcal{S}_0 = 2N_t(N_r - N_t + 1)/(N_r - N_t + 2)$, which are respectively identical with [35, Eq. (25)] and [35, Eq. (26)]. In the specific case of $N_t = 1$, the slope particularizes to $\mathcal{S}_0 = 2N_r/(N_r+1)$ which coincides with the associated results for both MMSE [32, Eq. (52)], [35, Eq. (24)] and optimal receivers [34, Eq. (16)]. This confirms that ZF detection becomes optimal for a single transmit antenna since all N_r degrees of freedom are devoted to the recovery of the corresponding multiplexed stream. All these results further demonstrate that for a fixed N_r, increasing N_t may improve the wideband slope, but also increases the minimum energy per bit due to the additional power required to cancel out the extra interferers.

D. Tight Bounds on the Sum Rate

Since the analytical expression in Theorem 2 is given in terms of a Meijer's-G function, which is a general function with a rather hard practical interpretation, it is important to obtain tight upper and lower closed-form bounds on the achievable sum rate. By doing so, we can complement the previous exact and asymptotic results and draw interesting insights on the impact of the system parameters. We begin with the following theorem which returns a novel, tight upper bound on the sum rare of ZF detectors:

Theorem 3: The achievable sum rate of ZF detectors over correlated K MIMO channels in (12) is upper bounded by

$$R \leq R_U = \sum_{m=1}^{LN_t} \log_2 \left(1 + \frac{\rho(N_r - LN_t + 1)}{LN_t} \frac{k_m \Omega_m}{\sigma_m D_m^{\upsilon}}\right). \tag{34}$$

Proof: The proof follows by applying Jensen's inequality on (12) along with the methodology of Corollary 3. ∎

Corollary 4: In the high-SNR regime, the upper bound in (34) becomes

$$R_U^{\infty} = LN_t \log_2\left(\frac{\rho}{LN_t}\right) + LN_t \log_2(N_r - LN_t + 1) - \sum_{m=1}^{LN_t} \log_2(\sigma_m) + N_t \sum_{m=1}^{L} \left(\log_2(k_m) + \log_2\left(\frac{\Omega_m}{D_m^{\upsilon}}\right)\right) \tag{35}$$

while the *high-SNR bound offset* is given by

$$\begin{aligned}\Delta R^{\infty} &\triangleq R_U^{\infty} - R^{\infty} \\ &= \frac{LN_t}{\ln 2}\left(\ln(N_r - LN_t + 1) - \psi(N_r - LN_t + 1)\right) \\ &\quad + \frac{N_t}{\ln 2}\sum_{m=1}^{L}\left(\ln(k_m) - \psi(k_m)\right).\end{aligned} \tag{36}$$

Interestingly, the upper bound becomes tighter for higher N_r, k_m. In the limit, $N_r, k_m \to \infty$, it converges to the exact high-SNR sum rate (i.e. $\Delta R^{\infty} \to 0$) since $\psi(x) \approx \ln(x)$ if $x \to \infty$ [27, Eq. (6.3.18)]. On a similar basis, we can now propose the following new lower bound on the sum rate:

Theorem 4: The achievable sum rate of ZF detectors over correlated K MIMO channels in (12) is lower bounded by

$$R \geq R_L = \sum_{m=1}^{LN_t} \log_2\left(1 + \frac{\rho}{LN_t}\exp\left(\psi\left(N_r - LN_t + 1\right) + \psi\left(k_m\right) + \ln\left(\frac{\Omega_m}{\sigma_m D_m^{\upsilon}}\right)\right)\right). \tag{37}$$

Proof: The proof relies on the generic bounding technique, originally proposed in [2, Theorem 1]. Omitting explicit details, we can directly lower bound (12) according to

$$R \geq R_L = \sum_{m=1}^{LN_t} \log_2\left(1 + \frac{\rho}{LN_t}\exp\left(\mathbb{E}\left[\ln\left(\frac{\xi_m x_m}{D_m^{\upsilon}}\right)\right]\right)\right) \tag{38}$$

where we have used the fact that $\log_2(1+\alpha\exp(x))$ is convex in x for $\alpha > 0$. Evaluating the expectation in (38), following the methodology of Corollary 2, and after factorization we conclude the proof. ∎

Comparing (16) with (37), we can see that the lower bound becomes exact at high-SNRs. Note that similar observations were also made in [2].

IV. SER and Outage Probability

A. Symbol Error Rate Analysis

We now analyze the SER performance of the ZF detectors introduced in Section II. To this end, we first invoke that for many modulation formats (e.g. BPSK, M-ary PSK, M-ary PAM) the average SER of the m-th subchannel (marginal SER) can be represented by the following generic formula [36]

$$\text{SER}_m = \mathbb{E}_{\gamma_m}\left[\alpha_m Q\left(\sqrt{2\beta_m\gamma_m}\right)\right], \quad m = 1, \ldots, LN_t \tag{39}$$

where $Q(\cdot)$ is the Gaussian Q-function while α_m, β_m are modulation-specific constants. For instance, for BPSK modulation ($\alpha_m = 1, \beta_m = 1$) while for M-ary PSK $\alpha_m = 2, \beta_m = \sin^2(\pi/M)$ [36, Eq. (5.2.61)]. The following theorem returns an analytical expression for the exact subchannel SER:

Theorem 5: The average SER of the m-th subchannel of a ZF detector over correlated K MIMO channels is

$$\text{SER}_m = \frac{a_m}{2\sqrt{\pi}\,(N_r - LN_t)!\,\Gamma(k_m)} \times G_{3,2}^{2,2}\left[\frac{\rho\Omega_m\beta_m}{LN_t D_m^{\upsilon}\sigma_m}\,\middle|\, \begin{matrix} LN_t - N_r, 1 - k_m, 1 \\ 0, \frac{1}{2}\end{matrix}\right]. \tag{40}$$

Proof: The proof starts by re-expressing (39) in terms of the complementary error function $\text{erfc}(\cdot)$, as follows

$$\begin{aligned}\text{SER}_m &= \frac{a_m}{2}\mathbb{E}_{\gamma_m}\left[\text{erfc}\left(\sqrt{\beta_m\gamma_m}\right)\right] \\ &= \frac{a_m}{2}\int_0^{\infty}\text{erfc}\left(\sqrt{\beta_m\gamma_m}\right) f_{\gamma_m}(\gamma_m)\, d\gamma_m\end{aligned} \tag{41}$$

where we have used the property $Q(x) = 0.5\text{erfc}\left(x/\sqrt{2}\right)$. Substituting (7) into (41), we get the desired result after expressing the $\text{erfc}(\cdot)$ integrand as [37, Eq. (8.4.14.2)]

$$\text{erfc}\left(\sqrt{x}\right) = \frac{1}{\sqrt{\pi}} G_{1,2}^{2,0}\left[x\,\middle|\, \begin{matrix} 1 \\ 0, \frac{1}{2}\end{matrix}\right] \tag{42}$$

and thereafter applying [25, Eq. (7.821.3)] to solve the resulting integral. ∎

Note that the marginal SER can be alternatively expressed via an infinite series, for $k_m \notin \mathbb{Z}$, as in (68) (see Appendix C). For the case that $N_r = LN_t$ and $k_m \notin \mathbb{Z}$, (40) simplifies via [38, Eq. (07.34.03.0897.01)] to (43) given at the top of the next page. By interchanging the order of the arguments in the hypergeometric functions in (43) and thereafter using [38, Eq. (07.25.03.0006.01)] and [38, Eq. (07.25.03.0002.01)] respectively, (43) becomes (44), where we have successively used Euler's reflection formula $\pi/\sin(\pi x) = \Gamma(x)\Gamma(1-x)$ [27, Eq. (6.1.17)] to simplify.

Apart from the marginal subchannel SER, an equally important measure of performance is the global average SER; for the considered case with independent symbols being sent over each subchannel, this can be directly expressed as

$$\text{SER} \triangleq \frac{1}{LN_t}\sum_{m=1}^{LN_t}\text{SER}_m. \tag{45}$$

$$\mathrm{SER}_m = \frac{a_m\sqrt{\pi}\csc\left(\pi\left(k_m-1\right)\right)}{2\Gamma\left(k_m\right)}\left(\frac{\frac{\sqrt{\pi}}{2}\frac{LN_tD_m^{\upsilon}\sigma_m}{\rho\Omega_m\beta_m}{}_2F_2\left(1,\frac{3}{2};2-k_m,2;\frac{LN_tD_m^{\upsilon}\sigma_m}{\rho\Omega_m\beta_m}\right)}{\Gamma\left(2-k_m\right)}\right.$$
$$\left.-\frac{\Gamma\left(k_m+\frac{1}{2}\right)\left(\frac{LN_tD_m^{\upsilon}\sigma_m}{\rho\Omega_m\beta_m}\right)^{k_m}{}_2F_2\left(k_m,k_m+\frac{1}{2};k_m,k_m+1;\frac{LN_tD_m^{\upsilon}\sigma_m}{\rho\Omega_m\beta_m}\right)}{\Gamma\left(k_m+1\right)}\right). \tag{43}$$

$$\mathrm{SER}_m = \frac{a_m}{2}\left(1-{}_1F_1\left(\frac{1}{2};1-k_m;\frac{LN_tD_m^{\upsilon}\sigma_m}{\rho\Omega_m\beta_m}\right)+\frac{\Gamma\left(1-k_m\right)\Gamma\left(k_m+\frac{1}{2}\right)}{\sqrt{\pi}\Gamma\left(k_m+1\right)}\right.$$
$$\left.\times\left(\frac{LN_tD_m^{\upsilon}\sigma_m}{\rho\Omega_m\beta_m}\right)^{k_m}{}_1F_1\left(k_m+\frac{1}{2};k_m+1;\frac{LN_tD_m^{\upsilon}\sigma_m}{\rho\Omega_m\beta_m}\right)\right). \tag{44}$$

To gain more insights, it is meaningful to explore the SER at high SNRs where the two critical measures characterizing the system performance are the diversity order and array (or coding) gain [39]:

Theorem 6: The average SER of the m-th subchannel of a ZF detector over correlated K MIMO channels at high SNRs and for $k_m \notin \mathbb{Z}$ is

$$\mathrm{SER}_m^{\infty} = \left(G_a(m)\rho\right)^{-G_d(m)} + o\left(\rho^{-G_d(m)}\right) \tag{46}$$

where we have defined $p \triangleq \min\left\{N_r - LN_t + 1, k_m\right\}$, $q \triangleq \max\left\{N_r - LN_t + 1, k_m\right\}$, while the diversity order and array gain are respectively

$$G_d(m) = p \tag{47}$$

$$G_a(m) = \frac{\Omega_m}{LN_tD_m^{\upsilon}\sigma_m}\left(\frac{a_m}{2\sqrt{\pi}\beta_m^p}\frac{\Gamma\left(q-p\right)\Gamma\left(p+\frac{1}{2}\right)}{\Gamma\left(p+1\right)\Gamma\left(q\right)}\right)^{-\frac{1}{p}}. \tag{48}$$

Proof: A detailed proof is given in Appendix C. ∎

We emphasize the fact that Theorem 6 implicitly requires that $k_m \notin \mathbb{Z}$ since for this case a series expansion of the modified Bessel function in (7) does not seem to be available in the literature (see (62) and discussion thereof). In any case though, this condition is not stringent and can be fulfilled by inserting an infinitely small perturbation term ϵ so that $(N_r - LN_t - k_m + 1 + \epsilon) \notin \mathbb{Z}$, when $k_m \in \mathbb{Z}$. More importantly, the above parametrization indicates that the diversity order depends only on the system dimensions and the shape parameter of gamma shadowing and, consequently, is independent of the terminal distances and the scale parameter of shadowing, Ω_m.

B. Outage Probability Analysis

For the case of non-ergodic channels (e.g. quasi-static or block-fading), it is more appropriate to resort to the notion of outage probability to characterize the performance of MIMO ZF detectors operating in K fading channels. In general, the outage probability is a critical measure of system performance and is defined as the probability that the instantaneous received SNR, γ_m, falls below a predefined threshold γ_{th}. Clearly, the outage probability can be directly obtained via the SNR CDF expressions in (8)–(10). In particular, we can express the outage probability of the m-th subchannel of a ZF detector according to

$$P_{\mathrm{out},m} \triangleq \Pr\left(\gamma_m \le \gamma_{\mathrm{th}}\right) = F_{\gamma_m}\left(\gamma_{\mathrm{th}}\right), \quad m = 1,\ldots,LN_t. \tag{49}$$

Since we are typically interested in small outage (e.g. 0.01, 0.001), we can exploit the outage performance for small γ_{th}. The following theorem returns the outage probability in the high-SNR regime:

Theorem 7: The outage probability of the m-th subchannel ($m = 1,\ldots,LN_t$) of a ZF detector over correlated K MIMO channels at high SNRs and for $k_m \notin \mathbb{Z}$ is

$$P_{\mathrm{out},m}^{\infty} = \frac{\Gamma\left(q-p\right)}{\Gamma\left(p+1\right)\Gamma(q)}\left(\frac{LN_tD_m^{\upsilon}\sigma_m}{\rho\Omega_m}\gamma_{\mathrm{th}}\right)^p + o\left(\gamma_{\mathrm{th}}^p\right). \tag{50}$$

Proof: The proof follows by applying a similar methodology as for the SER asymptotic results presented in Theorem 6. Hence, by integrating (63) to get the CDF according to $F_{\gamma_m}\left(\gamma_{\mathrm{th}}\right) = \int_0^{\gamma_{\mathrm{th}}} f_{\gamma_m}\left(\gamma_m\right) d\gamma_m$ and keeping only the dominant term in the resulting expression, (50) is obtained. ∎

V. Numerical Results

In this section, the theoretical analysis presented in Sections III and IV is validated through a set of Monte-Carlo simulations. We first generate 20,000 random realizations of the small and large-scale fading matrices $\mathbf{H}$ and $\boldsymbol{\Xi}$ according to (2), and thereafter obtain the simulated sum rate via (12). The transmit correlation matrix is constructed as $\mathbf{R}_t = \mathrm{diag}\left\{\mathbf{R}_{t,m}\right\}_{m=1}^{L}$ where $\mathbf{R}_{t,m}$ is the correlation matrix between the antennas of the m-th port. The entries of the latter are modeled via the common exponential correlation model $\left\{\mathbf{R}_{t,m}\right\}_{i,j} = \rho_{t,m}^{|i-j|}$ with $\rho_{t,m} \in [0,1)$ being the transmit correlation coefficient [40].

In Fig. 1, the achievable sum rate is plotted against the average SNR, ρ. For the sake of simplicity, we have set $k_m = 1, \Omega_m = 2, \rho_{t,m} = 0.3,\ \forall m = 1,\ldots,L$ while we consider different MIMO configurations by keeping $N_t = 2$ and increasing only N_r. The outputs of a Monte-Carlo simulator are compared with the exact analytical expression of Theorem 2 and the upper/lower bounds of (34) and (37), respectively. It is easily observed that the match between theory and simulation

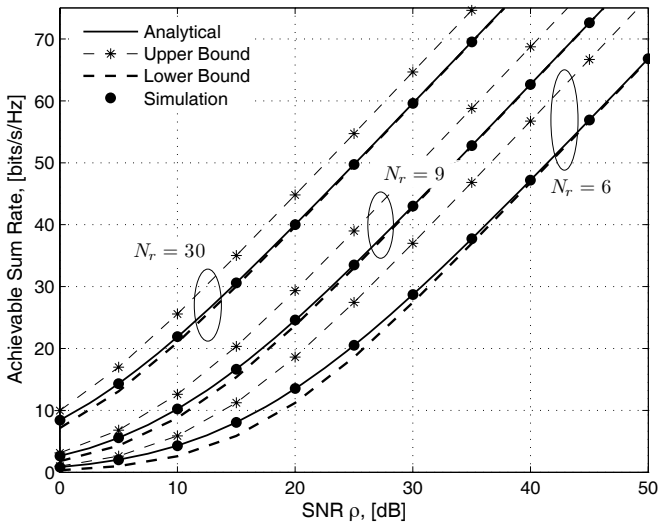

Fig. 1. Simulated sum rate, analytical expression and upper/lower bounds against the SNR ($N_t = 2$, $L = 3$, $\rho_{t,m} = 0.3$, $\upsilon = 4$, $k_m = 1$, $\Omega_m = 2$, $D_1 = 1000$ m, $D_2 = 1500$ m, $D_3 = 2000$ m).

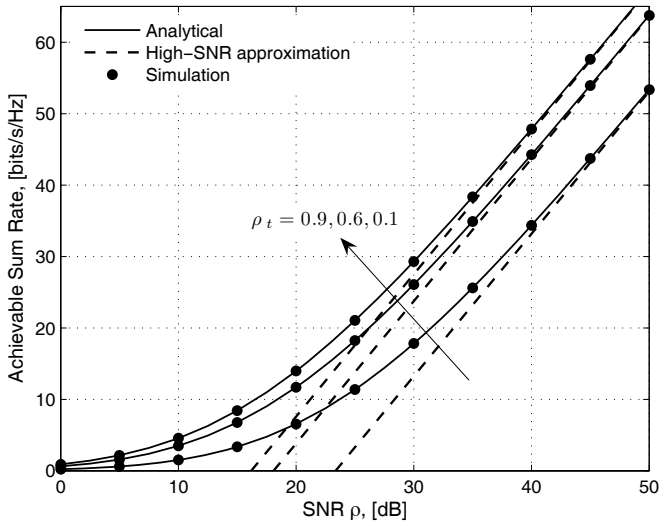

Fig. 2. Simulated sum rate, analytical expression and high-SNR approximation against the SNR ($N_r = 6$, $N_t = 2$, $L = 3$, $\upsilon = 4$, $k_m = 1$, $\Omega_m = 2$, $D_1 = 1000$ m, $D_2 = 1500$ m, $D_3 = 2000$ m).

is excellent in all cases under consideration, thereby validating the correctness of the proposed analytical expressions. The graph indicates that adding more receive antennas significantly stabilizes the MIMO link by improving the receive diversity and reducing the noise enhancement effect. This is consistent with the results in [19], [28]. Further, a higher N_r makes both bounds tighter although the upper bound is in general less tight due to the loose nature of Jensen's inequality. As previously mentioned, at high SNRs the lower bound becomes exact.

In Fig. 2, the effects of spatial correlation of the Rayleigh component, $\rho_{t,m} = \rho_t$, on sum rate are investigated with the high-SNR approximation curves being generated via (16). As anticipated, spatial correlation limits the advantages of MIMO technology due to the reduced diversity. In other words, the signatures of the impinging wavefronts become identical with a higher ρ_t, thereby decreasing the degrees of freedom of the MIMO channel. Spatial correlation has a minor effect at low and moderate SNRs, while its impact becomes far more pronounced as the SNR gets higher. Similar conclusions were also drawn in [4]. Interestingly, the high-SNR approximation becomes tight more slowly for a high ρ_t because of the increased spread of the subchannel SNRs (i.e. the weakest SNR becomes much smaller than the dominant one for high correlation levels). In any case though, the high-SNR expressions seem to become sufficiently tight even for moderate SNR values. This implies that they can explicitly predict the exact sum rate for most practical SNR values with a much lower computational load.

In Fig. 3, the analytical and simulated low-SNR sum rate are depicted against the transmit energy per bit E_b/N_0 (Proposition 2). For illustration purposes, we consider only small-scale fading (both correlated and i.i.d. Rayleigh fading). It can be observed that increasing N_t increases the minimum energy per bit and so does the correlation coefficient ρ_t. The wideband slope is enhanced with a higher N_t and seems to remain relatively unaffected by spatial correlation. For all scenarios under consideration, it turns out that the linear approximations

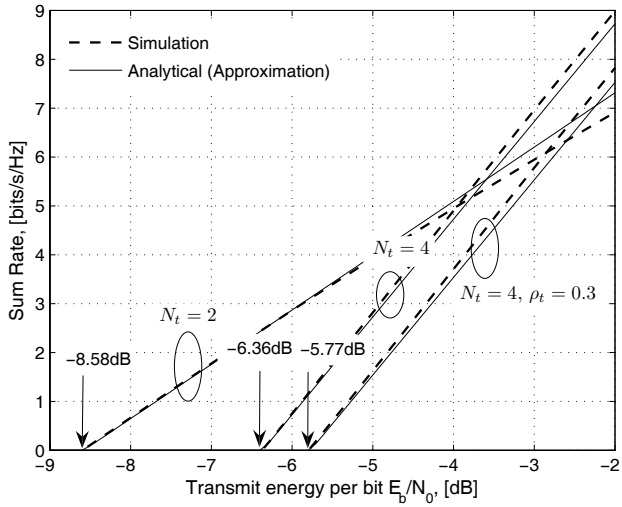

Fig. 3. Low-SNR simulated sum rate and analytical linear approximation against the transmit energy per bit ($N_r = 6$).

are quite accurate over a moderate range of E_b/N_0 values.

In Fig. 4, the exact subchannel/global SER curves based on (40) and (45) are overlaid with the output of a Monte-Carlo simulator. In addition, high-SNR curves generated via (46) are also presented. All subchannels are using QPSK modulation with modulation parameters $\alpha_m = 2$, $\beta_m = 0.5$. The graph indicates that the analytical expressions coincide with simulation results and likewise that the diversity order and array gains are accurately predicted. Moreover, the global average SER is quite close to the marginal SER of the third subchannel which corresponds to the medium transmitter-receiver distance ($L = 2$, $D_2 = 1500$ m).

In Fig. 5, the effects of the slow-fading parameters on the marginal SER are assessed. To this end, we consider a 6×2 MIMO configuration and the SER of the dominant subchannel, corresponding to the smallest transmitter-receiver distance (i.e. $D_1 = 1000$ m), is plotted for increasing values of the shape parameter k_1. It is clearly observed that a high k_1 diminishes

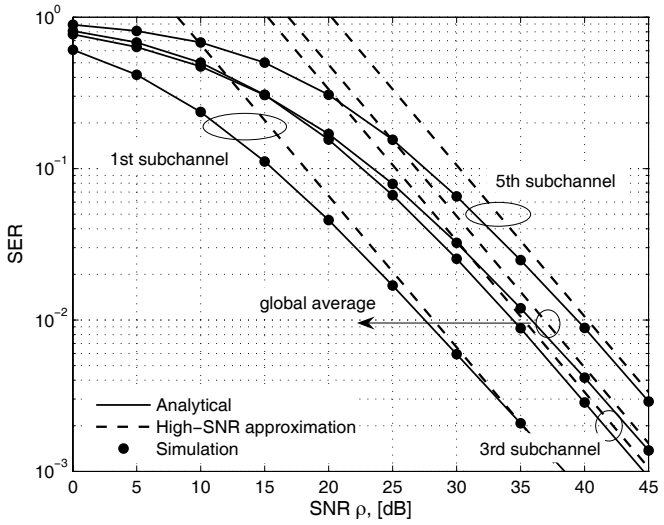

Fig. 4. Simulated subchannel/global average SER, analytical expression and high-SNR approximation against the SNR ($N_r = 6$, $N_t = 2$, $L = 3$, $\rho_{t,m} = 0.3$, $\upsilon = 4$, $k_m = 1.5$, $\Omega_m = 2$, $D_1 = 1000$ m, $D_2 = 1500$ m, $D_3 = 2000$ m).

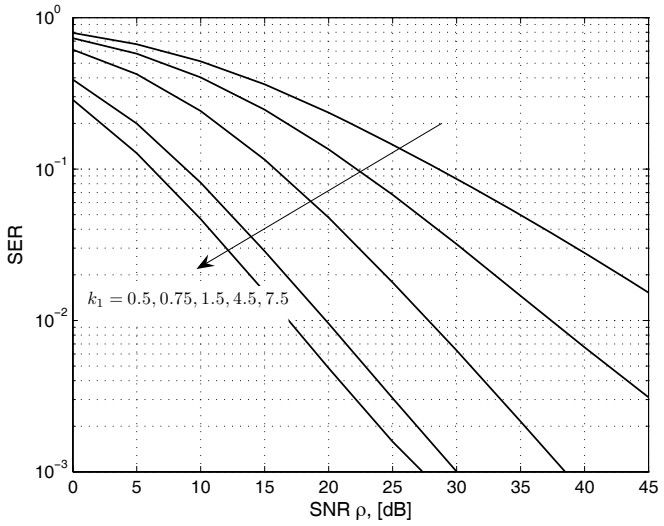

Fig. 5. Dominant subchannel SER against the SNR ($N_r = 6$, $N_t = 2$, $L = 3$, $\rho_{t,m} = 0.3$, $\upsilon = 4$, $\Omega_m = 2$, $D_1 = 1000$ m, $D_2 = 1500$ m, $D_3 = 2000$ m).

the effects of shadowing, thereby delivering smaller SER. However, the gap between the corresponding curves decreases as k_1 gets larger which implies that its effect becomes less pronounced; we recall that consistent conclusions were also drawn in [26] while, although not shown herein, our simulation results have indicated a similar trend in terms of sum rate as well.

Finally, Fig. 6 addresses the individual subchannel outage probability against the SNR, ρ, for a fixed threshold value $\gamma_{\text{th}} = 0.5$. The analytical and high-SNR approximation curves have been respectively generated via (49) and (50). Once more, there is an exact agreement between the analytical curves and the Monte-Carlo simulations. Note that the high-SNR approximations become exact even at a target outage of 10^{-2}, while an increase in SNR pronounces the difference in outage between the dominant subchannel and the weakest

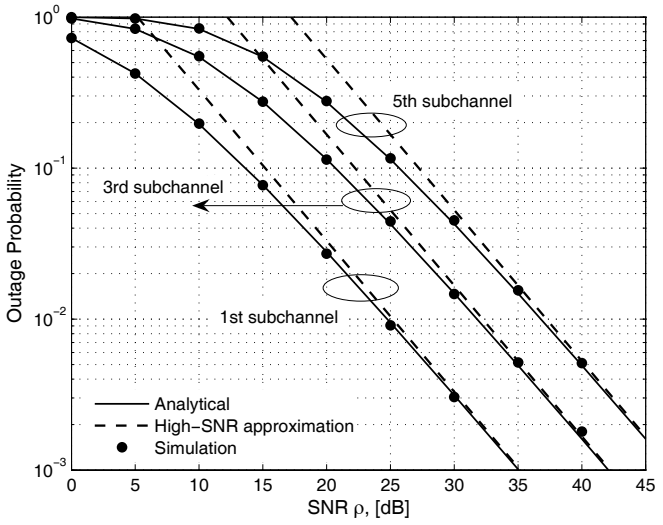

Fig. 6. Simulated subchannel outage probability, analytical expression and high-SNR approximation against the SNR ($N_r = 6$, $N_t = 2$, $L = 3$, $\rho_{t,m} = 0.3$, $\upsilon = 4$, $k_m = 1.5$, $\Omega_m = 2$, $\gamma_{\text{th}} = 0.5$, $D_1 = 1000$ m, $D_2 = 1500$ m, $D_3 = 2000$ m).

ones. We recall that the latter correspond to higher terminal distances and as such experience stronger path-loss attenuation.

VI. Conclusion

In this paper, a detailed statistical characterization of ZF detectors over correlated K MIMO channels was presented. After deriving analytical expressions for the PDF and CDF of the instantaneous subchannel SNR, we provided a novel formula for the exact achievable sum rate of the system under investigation. In parallel, tractable closed-form approximations were deduced in the asymptotically high and low-SNR regimes. Simple closed-form upper and lower bounds were also provided, which were demonstrated to remain tight across the entire SNR range. These expressions offer useful insights into the factors that govern the ZF detectors' performance. Our analysis validated the common belief that increasing the number of receive antennas has a beneficial effect on the ZF performance due to the additional degrees of freedom that enhance the spatial diversity and mitigate the noise enhancement effect.

In the second part of the paper, our main focus was on the marginal/global SER and outage probability characterization of the considered configurations. Exact expressions for both measures were given in analytical form along with first-order expansions around the origin. In addition, we quantified the asymptotic SER performance in terms of diversity order and array gain. We finally examined via numerical simulations, the implications of the model parameters on the overall performance of ZF detectors.

Appendix A
Proof of Theorem 1 and Corollary 1

The proof starts by defining $z_m = x_m \xi_m$, whose PDF can be evaluated according to

$$f_{z_m}(y) = \int_0^\infty \frac{1}{x} f_{x_m}(x) f_{\xi_m}\left(\frac{y}{x}\right) dx$$

$$F_{\gamma_m}(\gamma_{\text{th}}) = \int_0^{\gamma_{\text{th}}} f_{\gamma_m}(\gamma_m)\, d\gamma_m \tag{54}$$

$$= \frac{1}{(N_r - LN_t)!\Gamma(k_m)} \left(\frac{LN_t D_m^v \sigma_m}{\rho \Omega_m}\right)^{\frac{N_r - LN_t + k_m + 1}{2}} \times \int_0^{\gamma_{th}} \gamma_m^{\frac{N_r - LN_t + k_m - 1}{2}} G_{0,2}^{2,0}\left[\frac{LN_t D_m^v \sigma_m \gamma_m}{\rho \Omega_m}\,\middle|\, \begin{matrix} - \\ \frac{N_r - LN_t - k_m + 1}{2}, -\frac{N_r - LN_t - k_m + 1}{2} \end{matrix}\right] d\gamma_m \tag{55}$$

$$= \frac{1}{(N_r - LN_t)!\Gamma(k_m)} \left(\frac{LN_t D_m^v \sigma_m \gamma_{\text{th}}}{\rho \Omega_m}\right)^{\frac{N_r - LN_t + k_m + 1}{2}} \times G_{1,3}^{2,1}\left[\frac{LN_t D_m^v \sigma_m \gamma_{\text{th}}}{\rho \Omega_m}\,\middle|\, \begin{matrix} 1 - \frac{N_r - LN_t + k_m + 1}{2} \\ \frac{N_r - LN_t + 1 - k_m}{2}, -\frac{N_r - LN_t + 1 - k_m}{2}, -\frac{N_r - LN_t + k_m + 1}{2} \end{matrix}\right]. \tag{56}$$

$$= \frac{\sigma_m^{N_r - LN_t + 1}}{(N_r - LN_t)!} \frac{y^{k_m - 1}}{\Gamma(k_m)\Omega_m^{k_m}} \times \int_0^{\infty} \exp\left(-\sigma_m x - \frac{y}{\Omega_m x}\right) x^{N_r - LN_t - k_m} dx \tag{51}$$

$$= \frac{2}{(N_r - LN_t)!\Gamma(k_m)} \left(\frac{\sigma_m}{\Omega_m}\right)^{\frac{N_r - LN_t + k_m + 1}{2}} \times y^{\frac{N_r - LN_t + k_m - 1}{2}} K_{N_r - LN_t - k_m + 1}\left(2\sqrt{\frac{\sigma_m}{\Omega_m} y}\right) \tag{52}$$

where from (51) to (52) we have used [25, Eq. (3.471.9)]. The desired expression in (7) is then readily obtained via the following change of variables

$$f_{\gamma_m}(\gamma_m) = \frac{LN_t D_m^v}{\rho} f_{z_m}\left(\frac{LN_t D_m^v \gamma_m}{\rho}\right) \tag{53}$$

and some basic algebra. For the CDF expression in (8), we can express $F_{\gamma_m}(\gamma_{\text{th}}) = \Pr(\gamma_m \le \gamma_{\text{th}})$ through (54)–(56). From (54) to (55) we have used (7) and the Meijer's-G representation of the Bessel function from [41, Eq. (14)], while from (55) to (56) we employ a useful integral identity from [41, Eq. (26)]. The proof concludes after applying the following property of Meijer's-G functions [25, Eq. (9.31.5)] on (56)

$$z^k G_{p,q}^{m,n}\left[z\,\middle|\, \begin{matrix} \mathbf{a}_p \\ \mathbf{b}_q \end{matrix}\right] = G_{p,q}^{m,n}\left[z\,\middle|\, \begin{matrix} \mathbf{a}_p + k \\ \mathbf{b}_q + k \end{matrix}\right].$$

Appendix B
Proof of Corollary 1

In order to deduce the alternative expression in (9), we simply need to expand the Meijer's-G function in (8) in terms of hypergeometric function according to [38, Eq. (07.34.03.0727.01)]. This a standard methodology that can be applied as long as the arguments of a Meijer's-G function are not integers [25], [38]. For the expression in (10), we set to find a generic closed-form solution for integrals of the type

$$F_{\gamma_m}(\gamma_{\text{th}}) = \frac{4\omega^{\frac{a+b}{2}}}{(a-1)!\Gamma(b)} \int_0^{\sqrt{\gamma_{\text{th}}}} y^{a+b-1} K_{a-b}\left(2\sqrt{\omega} y\right) dy \tag{57}$$

where $a = N_r - LN_t + 1$, $b = k_m$ and $\omega = \frac{LN_t D_m^v \sigma_m}{\rho \Omega_m}$. Using the fact that [25, Eq. (8.486.14)]

$$\frac{d}{dz}\left(z^{\nu} K_{\nu}(az)\right) = -a z^{\nu} K_{\nu - 1}(az)$$

(57) can be rewritten as

$$F_{\gamma_m}(\gamma_{\text{th}}) = -\frac{2\omega^{\frac{a+b-1}{2}}}{(a-1)!\Gamma(b)} \times \int_0^{\sqrt{\gamma_{\text{th}}}} y^{2b-2} \frac{d}{dy}\left(y^{a-b+1} K_{a-b+1}\left(2\sqrt{\omega} y\right)\right) dy$$

and by integration by parts we get

$$F_{\gamma_m}(\gamma_{\text{th}}) = -\frac{2\omega^{\frac{a+b-1}{2}}}{(a-1)!\Gamma(b)} \gamma_{\text{th}}^{\frac{a+b-1}{2}} K_{a-b+1}\left(2\sqrt{\omega \gamma_{\text{th}}}\right) + \frac{4\omega^{\frac{a+b-1}{2}}(b-1)}{(a-1)!\Gamma(b)} \int_0^{\sqrt{\gamma_{\text{th}}}} y^{a+b-2} K_{a-b+1}\left(2\sqrt{\omega} y\right) dy. \tag{58}$$

Clearly, the derivation now requires the analytical evaluation of the integral

$$\mathcal{I}(a, \omega, \ell) = \int_0^{\sqrt{\gamma_{\text{th}}}} y^{a+\ell} K_{a-\ell-1}\left(2\sqrt{\omega} y\right) dy$$
$$= \int_0^{\sqrt{\gamma_{\text{th}}}} \left(-\frac{y^{2\ell}}{2\sqrt{\omega}}\right) \frac{d}{dy}\left(y^{a-\ell} K_{a-\ell}\left(2\sqrt{\omega} y\right)\right) dy$$
$$= -\left[\frac{y^{2\ell}}{2\sqrt{\omega}} y^{a-\ell} K_{a-\ell}\left(2\sqrt{\omega} y\right)\right]_0^{\sqrt{\gamma_{\text{th}}}} + \frac{\ell}{\sqrt{\omega}} \int_0^{\sqrt{\gamma_{\text{th}}}} y^{a+\ell-1} K_{a-\ell}\left(2\sqrt{\omega} y\right) dy$$
$$= -\frac{1}{2\sqrt{\omega}} \gamma_{\text{th}}^{\frac{\ell+a}{2}} K_{a-\ell}\left(2\sqrt{\omega \gamma_{\text{th}}}\right) + \lim_{y \to 0} \frac{y^{2\ell}}{2\sqrt{\omega}} y^{a-\ell} K_{a-\ell}\left(2\sqrt{\omega} y\right) + \frac{\ell}{\sqrt{\omega}} \mathcal{I}(a, \omega, \ell - 1). \tag{59}$$

The second term in (59) can be evaluated according to [27, Eq. (9.6.9)]

$$K_{\nu}(z) \overset{z \to 0}{\approx} \frac{\Gamma(\nu)}{2} \left(\frac{2}{z}\right)^{\nu}, \quad \text{Re}(\nu) > 0$$

which when plugged into (59) leads to

$$\mathcal{I}(a, \omega, \ell) = -\frac{1}{2\sqrt{\omega}} \gamma_{\text{th}}^{\frac{\ell+a}{2}} K_{a-\ell}\left(2\sqrt{\omega \gamma_{\text{th}}}\right) + \frac{\Gamma(a-\ell)}{4\omega^{\frac{a-\ell+1}{2}}} \lim_{y \to 0} y^{2\ell} + \frac{\ell}{\sqrt{\omega}} \mathcal{I}(a, \omega, \ell - 1)$$
$$= -\frac{1}{2\sqrt{\omega}} \gamma_{\text{th}}^{\frac{\ell+a}{2}} K_{a-\ell}\left(2\sqrt{\omega \gamma_{\text{th}}}\right) + \frac{\ell}{\sqrt{\omega}} \mathcal{I}(a, \omega, \ell - 1). \tag{60}$$

$$\mathrm{SER}_m = \frac{a_m}{(N_r - LN_t)!\Gamma(k_m)\sin(\pi(N_r - LN_t + 1 - k_m))} \times \left(\sum_{\ell=0}^{\infty} \frac{\left(\frac{LN_t D_m^v \sigma_m}{\rho\Omega_m}\right)^{\ell+k_m} \int_0^{\frac{\pi}{2}} \int_0^{\infty} \gamma_m^{\ell+k_m-1} \exp\left(-\frac{\beta_m \gamma_m}{\sin^2\theta}\right) d\gamma_m d\theta}{\ell!\Gamma(\ell - N_r + LN_t + k_m)} - \sum_{\ell=0}^{\infty} \frac{\left(\frac{LN_t D_m^v \sigma_m}{\rho\Omega_m}\right)^{\ell+N_r-LN_t+1} \int_0^{\frac{\pi}{2}} \int_0^{\infty} \gamma_m^{\ell+N_r-LN_t} \exp\left(-\frac{\beta_m x}{\sin^2\theta}\right) d\gamma_m d\theta}{\ell!\Gamma(\ell + N_r - LN_t + 2 - k_m)} \right). \quad (64)$$

In a very similar manner, we can get for $\mathcal{I}(a,\omega,0)$ the following expression

$$\begin{aligned}\mathcal{I}(a,\omega,0) &= \int_0^{\sqrt{\gamma_{\mathrm{th}}}} y^a K_{a-1}\left(2\sqrt{\omega}y\right) dy \\ &= -\frac{1}{2\sqrt{\omega}} \int_0^{\sqrt{\gamma_{\mathrm{th}}}} \frac{d}{dy}\left(y^a K_a\left(2\sqrt{\omega}y\right)\right) dy \\ &= -\frac{\omega^{-\frac{a+1}{2}}}{2}(\omega\gamma_{\mathrm{th}})^{\frac{a}{2}} K_a\left(2\sqrt{\omega\gamma_{\mathrm{th}}}\right) + \lim_{y\to 0} \frac{y^a \Gamma(a)}{4\sqrt{\omega}} \left(\frac{1}{\sqrt{\omega}y}\right)^a \\ &= -\frac{\omega^{-\frac{a+1}{2}}}{2}(\omega\gamma_{\mathrm{th}})^{\frac{a}{2}} K_a\left(2\sqrt{\omega\gamma_{\mathrm{th}}}\right) + \frac{\omega^{-\frac{a+1}{2}}\Gamma(a)}{4}. \end{aligned} \quad (61)$$

Combining (58) with (60)–(61), we can conclude the proof as follows

$$\begin{aligned} F_{\gamma_m}(\gamma_{\mathrm{th}}) &= -\frac{2\omega^{\frac{a+b-1}{2}}}{(a-1)!\Gamma(b)} \gamma_{\mathrm{th}}^{\frac{a+b-1}{2}} K_{a-b+1}\left(2\sqrt{\omega\gamma_{\mathrm{th}}}\right) \\ &\quad + \frac{4\omega^{\frac{a+b-1}{2}}(b-1)}{(a-1)!\Gamma(b)} \mathcal{I}(a,\omega,b-2) \\ &= -\sum_{\ell=1}^{b-1} \frac{2\omega^{\frac{a+\ell}{2}}}{(a-1)!(b-\ell)!} \gamma_{\mathrm{th}}^{\frac{a+\ell}{2}} K_{a-\ell}\left(2\sqrt{\omega\gamma_{\mathrm{th}}}\right) \\ &\quad + \frac{4\omega^{\frac{a+1}{2}}}{(a-1)!} \mathcal{I}(a,\omega,0) \\ &= 1 - \sum_{\ell=0}^{b-1} \frac{2\omega^{\frac{a+\ell}{2}}}{(a-1)!(b-\ell)!} \gamma_{\mathrm{th}}^{\frac{a+\ell}{2}} K_{a-\ell}\left(2\sqrt{\omega\gamma_{\mathrm{th}}}\right). \end{aligned}$$

APPENDIX C
PROOF OF THEOREM 6

The proof starts by adopting the generalized power series expansion of the modified Bessel function of the second kind in (7), which originates by combining [27, Eq. (9.6.2)] with [27, Eq. (9.6.10)][3]

$$K_\nu(z) = \frac{\pi}{2\sin(\pi\nu)} \left(\sum_{\ell=0}^{\infty} \frac{1}{\ell!\Gamma(\ell-\nu+1)} \left(\frac{z}{2}\right)^{2\ell-\nu} - \sum_{\ell=0}^{\infty} \frac{1}{\ell!\Gamma(\ell+\nu+1)} \left(\frac{z}{2}\right)^{2\ell+\nu} \right). \quad (62)$$

Note that (62) holds for $\nu \notin \mathbb{Z}$ and $|z| < \infty$, which is evidently valid for most realistic scenarios under consideration. Combining (7) with (62) and after some factorization, we obtain

$$f_{\gamma_m}(\gamma_m) = \frac{\pi}{(N_r - LN_t)!\sin(\pi(N_r - LN_t + 1 - k_m))} \times \frac{1}{\Gamma(k_m)} \left(\sum_{\ell=0}^{\infty} \frac{\left(\frac{LN_t D_m^v \sigma_m}{\rho\Omega_m}\right)^{\ell+k_m} \gamma_m^{\ell+k_m-1}}{\ell!\Gamma(\ell - N_r + LN_t + k_m)} - \sum_{\ell=0}^{\infty} \frac{\left(\frac{LN_t D_m^v \sigma_m}{\rho\Omega_m}\right)^{\ell+N_r-LN_t+1} \gamma_m^{\ell+N_r-LN_t}}{\ell!\Gamma(\ell + N_r - LN_t + 2 - k_m)} \right). \quad (63)$$

As a next step, the alternative representation of the Gaussian Q-function is introduced in (39), which reads as $Q(x) = \frac{1}{\pi}\int_0^{\pi/2} \exp\left(-\frac{x^2}{2\sin^2\theta}\right) d\theta$ [13, Eq. (4.2)]. Then, the subchannel SER expression can be rewritten as in (64) at the top of the page.

The first double integral in (64) admits the following closed-form expression

$$\begin{aligned} &\int_0^{\frac{\pi}{2}} \int_0^{\infty} \gamma_m^{\ell+k_m-1} \exp\left(-\frac{\beta_m\gamma_m}{\sin^2\theta}\right) d\gamma_m d\theta \\ &= \frac{\Gamma(\ell+k_m)}{\beta_m^{\ell+k_m}} \int_0^{\frac{\pi}{2}} (\sin\theta)^{2\ell+2k_m} d\theta \quad (65) \\ &= \frac{\Gamma\left(\frac{1}{2}\right)}{2\beta_m^{\ell+k_m}} \frac{\Gamma(\ell+k_m)\Gamma\left(\ell+k_m+\frac{1}{2}\right)}{\Gamma(\ell+k_m+1)} \quad (66) \end{aligned}$$

where (65) stems from (26) while (66) is a result of [25, Eq. (3.621.1)]

$$\int_0^{\pi/2} \sin^{\mu-1} x dx = \frac{\Gamma\left(\frac{1}{2}\right)\Gamma\left(\frac{\mu}{2}\right)}{2\Gamma\left(\frac{\mu+1}{2}\right)}. \quad (67)$$

Following a similar line of reasoning for the second integral in (64), we end up with (68).

For large SNR, we only need to consider the smallest exponent of ℓ in (68), i.e. $\ell = 0$. Likewise, introducing the definitions of p and q and after factorization, we can finally approximate (68) with

$$\begin{aligned} \mathrm{SER}_m^{\infty} &= \frac{a_m \Gamma\left(\frac{1}{2}\right)}{2\Gamma(q)\Gamma(p)\sin(\pi(q-p))} \times \frac{\left(\frac{LN_t D_m^v \sigma_m}{\rho\Omega_m}\right)^p \Gamma(p)\Gamma\left(p+\frac{1}{2}\right)}{\beta_m^p \Gamma(p-q+1)\Gamma(p+1)} \quad (69) \\ &= \frac{a_m}{2\sqrt{\pi}\beta_m^p} \frac{\Gamma(q-p)\Gamma\left(p+\frac{1}{2}\right)}{\Gamma(q)\Gamma(p+1)} \left(\frac{LN_t D_m^v \sigma_m}{\rho\Omega_m}\right)^p \quad (70) \end{aligned}$$

[3]Please note that a similar analysis was recently reported in [42] in the context of free-space optical systems.

$$\mathrm{SER}_m = \frac{a_m \Gamma\left(\frac{1}{2}\right)}{(N_r - LN_t)!\Gamma\left(k_m\right)\sin\left(\pi\left(N_r - LN_t + 1 - k_m\right)\right)} \times \left(\sum_{\ell=0}^{\infty} \frac{\left(\frac{LN_t D_m^{\upsilon}\sigma_m}{\rho\Omega_m}\right)^{\ell+k_m} \frac{\Gamma(\ell+k_m)\Gamma\left(\ell+k_m+\frac{1}{2}\right)}{2\beta_m^{\ell+k_m}\Gamma(\ell+k_m+1)}}{\ell!\Gamma\left(\ell - N_r + LN_t + k_m\right)} - \sum_{\ell=0}^{\infty} \frac{\left(\frac{LN_t D_m^{\upsilon}\sigma_m}{\rho\Omega_m}\right)^{\ell+N_r-LN_t+1} \frac{\Gamma(\ell+N_r-LN_t+1)\Gamma\left(\ell+N_r-LN_t+\frac{3}{2}\right)}{2\beta_m^{\ell+N_r-LN_t+1}\Gamma(\ell+N_r-LN_t+2)}}{\ell!\Gamma\left(\ell + N_r - LN_t + 2 - k_m\right)} \right). \quad (68)$$

where from (69) to (70) we have used the property $\Gamma(1/2) = \sqrt{\pi}$ and Euler's reflection formula. This concludes the proof.

ACKNOWLEDGMENT

The authors would like to thank Prof. Matthew R. McKay, from Hong Kong University of Science and Technology, for his valuable help with the low-SNR capacity simulations.

REFERENCES

[1] I. E. Telatar, "Capacity of multi-antenna Gaussian channels," *Europ. Trans. Telecommun.*, vol. 10, no. 6, pp. 585–595, Nov./Dec. 1999.

[2] Ö. Oyman, R. Nabar, H. Bölcskei, and A. Paulraj, "Characterizing the statistical properties of mutual information in MIMO channels," *IEEE Trans. Signal Process.*, vol. 51, no. 11, pp. 2782–2795, Nov. 2003.

[3] A. Grant, "Rayleigh fading multi-antenna channels," *EURASIP J. Appl. Signal Process.*, vol. 2002, no. 3, pp. 316–329, Mar. 2002.

[4] H. Shin and J. H. Lee, "Capacity of multi-antenna fading channels: spatial fading correlation, double scattering, and keyhole," *IEEE Trans. Inf. Theory*, vol. 49, no. 10, pp. 2636–2647, Oct. 2003.

[5] M. Matthaiou, Y. Kopsinis, D. I. Laurenson, and A. M. Sayeed, "Upper bound for the ergodic capacity of dual MIMO Ricean systems: simplified derivation and asymptotic tightness," *IEEE Trans. Commun.*, vol. 57, no. 12, pp. 3589–3596, Dec. 2009.

[6] A. A. M. Saleh, A. J. Rustako, and R. S. Roman, "Distributed antennas for indoor radio environments," *IEEE Trans. Commun.* vol. 35, no. 12, pp. 1245–1252, Dec. 1987.

[7] M. V. Clark, *et al.*, "Distributed versus centralized antenna arrays in broadband wireless networks," in *Proc. IEEE Veh. Techn. Conf.*, May 2001, pp. 33–37.

[8] W. Roh and A. Paulraj, "Outage performance of the distributed antenna systems in a composite fading channel," in *Proc. IEEE Veh. Techn. Conf.*, Sep. 2002, vol. 3, pp. 1520–1524.

[9] H. Zhang and H. Dai, "On the capacity of distributed MIMO systems," in *Proc. Conf. Inform. Sciences and Systems*, Mar. 2004.

[10] H. Dai, "Distributed versus co-located MIMO systems with correlated fading and shadowing," in *Proc. IEEE Int. Conf. Acoustics Speech Signal Proc.*, May 2006.

[11] H. Dai, H. Zhang, and Q. Zhou, "Some analysis in distributed MIMO systems," *J. Commun.*, vol. 2, no. 3, pp. 43–50, May 2007.

[12] H. Suzuki, "A statistical model for urban radio propagation," *IEEE Trans. Commun.*, vol. 25, no. 7, pp. 673-680, July 1977.

[13] M. K. Simon and M.-S. Alouini, *Digital Communication over Fading Channels*, 2nd edition. John Wiley & Sons, 2005.

[14] L. S. Pillutla and S. K. Jayaweera, "Capacity of MIMO systems in Rayleigh fading and shadowing," in *Proc. Asilomar Conf. Signals, Systems Computers*, Nov. 2004, vol. 1, pp. 1149–1153.

[15] D. Wang, X. You, J. Wang, Y. Wang, and X. Hou, "Spectral efficiency of distributed MIMO cellular systems in a composite fading channel," in *Proc. IEEE Intern. Conf. Commun.*, May 2008, pp. 1259–1264.

[16] M. Park, C. B. Chae, and R. W. Heath, Jr., "Ergodic capacity of spatial multiplexing MIMO channels with log-normal shadowing and Rayleigh fading," in *Proc. IEEE Int. Symp. Personal Indoor Mobile Radio Commun.*, Sep. 2007.

[17] A. Abdi, H. A. Barger, and M. Kaveh, "A simple alternative to the lognormal model of shadow fading in terrestrial and satellite channels," in *Proc. IEEE Vehic. Technol. Conf.*, Oct. 2001, pp. 2058–2062.

[18] A. Abdi and M. Kaveh, "K distribution: an appropriate substitute for Rayleigh-lognormal distribution in fading-shadowing wireless channels," *IEE Electron. Lett.*, vol. 34, no. 9, pp. 851–852, Apr. 1998.

[19] A. Paulraj, R. Nabar, and D. A. Gore, *Introduction to Space-Time Wireless Communications*. Cambridge University Press, May 2003.

[20] D. A. Gore, R. W. Heath, Jr., and A. Paulraj, "Transmit selection in spatial multiplexing systems," *IEEE Commun. Lett.*, vol. 6, no. 11, pp. 491–493, Nov. 2002.

[21] H. Liu, Y. Song, and R. C. Qiu, "The impact of fading correlation on the error performance of MIMO systems over Rayleigh fading channels," *IEEE Trans. Wireless Commun.*, vol. 4, no. 5, pp. 2014–2019, Sep. 2005.

[22] M. Kiessling and J. Speidel, "Analytical performance of MIMO zero-forcing receivers in correlated Rayleigh fading environments," in *Proc. IEEE Signal Process. Advances Wireless Commun.*, June 2003, pp. 383–387.

[23] R. Xu and F. C. M. Lau, "Performance analysis for MIMO systems using zero-forcing detector over fading channels," *IEE Proc. Commun.*, vol. 153, no. 1, pp. 74–80, Feb. 2006.

[24] H. A. Abou Saleh and W. Hamouda, "Performance of zero-forcing detectors over MIMO flat-correlated Ricean fading channels," *IET Commun.*, vol. 3, no. 1, pp. 10–16, Jan. 2009.

[25] I. S. Gradshteyn and I. M. Ryzhik, *Table of Integrals, Series, and Products*, 7th edition. Academic Press, 2007.

[26] P. S. Bithas, N. C. Sagias, P. T. Mathiopoulos, G. K. Karagiannidis, and A. A. Rontogiannis, "On the performance analysis of digital communications over generalized-K fading channels," *IEEE Commun. Lett.*, vol. 10, no. 5, pp. 353–355, May 2006.

[27] M. Abramowitz and I. A. Stegun, *Handbook of Mathematical Functions with Formulas, Graphs, and Mathematical Tables*, 9th edition. Dover, 1970.

[28] C.-J. Chen and L.-C. Wang, "Performance analysis of scheduling in multiuser MIMO systems with zero-forcing receivers," *IEEE J. Sel. Areas Commun.*, vol. 25, no. 7, pp. 1435–1445, Sep. 2007.

[29] M. Matthaiou, N. D. Chatzidiamantis, G. K. Karagiannidis, and J. A. Nossek, "On the capacity of generalized-K fading MIMO channels," *IEEE Trans. Signal Process.*, vol. 58, no. 11, pp. 5939–5944, Nov. 2010.

[30] S. Shamai (Shitz) and S. Verdú, "The impact of frequency-flat fading on the spectral efficiency of CDMA," *IEEE Trans. Inf. Theory*, vol. 47, no. 4, pp. 1302–1327, May 2001.

[31] A. Lozano, A. M. Tulino, and S. Verdú, "High-SNR power offset in multiantenna communications," *IEEE Trans. Inf. Theory*, vol. 51, no. 12, pp. 4134–4151, Dec. 2005.

[32] M. R. McKay, I. B. Collings, and A. M. Tulino, "Achievable sum rate of MIMO MMSE receivers: a general analytic framework," *IEEE Trans. Inf. Theory*, vol. 56, no. 1, pp 396–410, Jan. 2010.

[33] S. Verdú, "Spectral efficiency in the wideband regime," *IEEE Trans. Inf. Theory*, vol. 48, no. 6, pp. 1319–1343, June 2001.

[34] A. Lozano, A. M. Tulino, and S. Verdú, "Multiple-antenna capacity in the low-power regime," *IEEE Trans. Inf. Theory*, vol. 49, no. 10, pp. 2527–2544, Oct. 2003.

[35] R. H. Y. Louie, M. R. McKay, and I. B. Collings, "Sum capacity of MIMO multiuser scheduling with linear receivers," *IEEE Trans. Commun.*, vol. 57, no. 11, pp. 3500–3510, Nov. 2009.

[36] J. G. Proakis, *Digital Communications*, 4th edition. McGraw-Hill, 2001.

[37] A. P. Prudnikov, Y. A. Brychkov, and O. I. Marichev, *Integrals and Series, Volume 3: More Special Functions*. Gordon and Breach, 1990.

[38] Wolfram, "The Wolfram functions site." Available: http://functions.wolfram.com

[39] Z. Wang and G. B. Giannakis, "A simple and general parameterization quantifying performance in fading channels," *IEEE Trans. Commun.*, vol. 51, no. 8, pp. 1389–1398, Aug. 2003.

[40] S. L. Loyka, "Channel capacity of MIMO architecture using the exponential correlation matrix," *IEEE Commun. Lett.*, vol. 5, no. 9, pp. 369–371, Sep. 2001.

[41] V. S. Adamchik and O. I. Marichev, "The algorithm for calculating integrals of hypergeometric type functions and its realization in REDUCE system," in *Proc. Intern. Conf. Symbolic Algebraic Computation*, 1990, pp. 212–224.

[42] E. Bayaki, R. Schober, and R. K. Mallik, "Performance analysis of MIMO free-space optical systems in gamma-gamma fading," *IEEE Trans. Commun.*, vol. 57, no. 9, pp. 3415–3424, Nov. 2009.

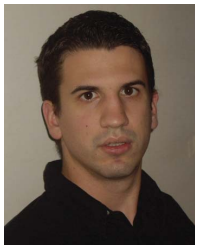

Michail Matthaiou (S'05-M'08) was born in Thessaloniki, Greece in 1981. He obtained the Diploma degree (5 years) in electrical and computer engineering from the Aristotle University of Thessaloniki, Greece in 2004. He then received the M.Sc. (with distinction) in communication systems and signal processing from the University of Bristol, U.K., and Ph.D. degrees from the University of Edinburgh, U.K. in 2005 and 2008, respectively. From September 2008 through May 2010, he was with the Institute for Circuit Theory and Signal Processing, Munich University of Technology (TUM), Germany, working as a Postdoctoral Research Associate. In June 2010, he joined Chalmers University of Technology, Gothenburg, Sweden, as an Assistant Professor. His research interests span signal processing for wireless communications, random matrix theory and multivariate statistics for MIMO systems, and performance analysis of fading channels.

Dr. Matthaiou is a co-recipient of the 2006 IEEE Communications Chapter Project Prize for the best M.Sc. dissertation in the area of communications.

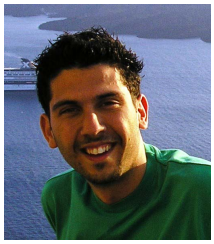

Nestor D. Chatzidiamantis (S'08) was born in Los Angeles, USA, in 1981. He received the Diploma degree (5 years) in electrical and computer engineering from the Aristotle University of Thessaloniki, Greece, and the M.Sc. award (with Distinction) in telecommunication networks and software from the University of Surrey, U.K. in 2005 and 2006, respectively. In November 2007, he joined again the ECE department of the Aristotle University of Thessaloniki, where he is pursuing a Ph.D degree.

His research areas span performance analysis of wireless communication systems over fading channels, communications theory, and free-space optical communications.

George K. Karagiannidis (M'97-SM'04) was born in Pithagorion, Samos Island, Greece. He received the University Diploma (5 years) and Ph.D degree, both in electrical and computer engineering, from the University of Patras, in 1987 and 1999, respectively. From 2000 to 2004, he was a Senior Researcher at the Institute for Space Applications and Remote Sensing, National Observatory of Athens, Greece. In June 2004, he joined Aristotle University of Thessaloniki, Thessaloniki, where he is currently an Associate Professor of Digital Communications Systems in the Electrical and Computer Engineering Department and Head of the Telecommunications Systems and Networks Lab.

His current research interests are in the broad area of digital communications systems with emphasis on cooperative communication, adaptive modulation, MIMO systems, optical wireless, and underwater communications. He is the author or co-author of more than 120 technical papers published in scientific journals and presented at international conferences. He is also a co-author of three chapters in books and author of the Greek edition book on telecommunications systems.

Dr. Karagiannidis has been a member of the Technical Program Committees for several IEEE conferences such as ICC, GLOBECOM, etc. He is a member of the editorial boards of the IEEE TRANSACTIONS ON COMMUNICATIONS, Senior Editor of IEEE COMMUNICATIONS LETTERS, and Lead Guest Editor of the special issue on "Optical Wireless Communications" of the IEEE JOURNAL ON SELECTED AREAS IN COMMUNICATIONS. He is co-recipient of the Best Paper Award of the Wireless Communications Symposium (WCS) in the IEEE International Conference on Communications (ICC'07), Glasgow, U.K., June 2007.

Dr. Karagiannidis is the Chair of the IEEE COMSOC Greek Chapter.

Josef A. Nossek (S'72-M'74-SM'81-F'93) received the Dipl.-Ing. and the Dr. techn. degrees in electrical engineering from the University of Technology in Vienna, Austria, in 1974 and 1980, respectively. In 1974, he joined Siemens AG in Munich, Germany, as a member of technical staff, in 1978 he became supervisor, and from 1980 on he was Head of Department. In 1987, he was promoted to Head of all radio systems design. Since 1989, he has been a Full Professor for circuit theory and signal processing at the Munich University of Technology, where he teaches undergraduate and graduate courses on circuit and systems theory and signal processing, and leads research on signal processing algorithms for communications. He was President Elect, President, and Past President of the IEEE Circuits and Systems Society in 2001, 2002, and 2003, respectively. He was Vice President of VDE (Verband der Elektrotechnik, Elektronik und Informationstechnik e.V.) in 2005 and 2006, President of VDE in 2007 and 2008, and was again Vice President of VDE in 2009 and 2010. His awards include the ITG Best Paper Award in 1988, the Mannesmann Mobilfunk (now Vodafone) Innovations Award in 1998, the Award for Excellence in Teaching from the Bavarian Ministry for Science, Research, and Art in 1998, and the Golden Jubilee Medal of the IEEE Circuits and Systems Society for 'Outstanding Contributions to the Society' in 1999. In 2008, he received the Education Award of the IEEE Circuits and Systems Society and the Order of Merit from the Federal Republic of Germany. Since 2009, he is Member of the National Academy of Engineering Sciences of Germany (acatech).